Journal of Applied Geophysics 129 (2016) 8–16

Contents lists available at ScienceDirect

Journal of Applied Geophysics

journal homepage: www.elsevier.com/locate/jappgeo

The optimal fractional S transform of seismic signal based on the normalized second-order central moment

Yuqing Wang, Zhenming Peng *

School of Optoelectronic Information, University of Electronic Science and Technology of China, Chengdu 610054, China

ARTICLE INFO

Article history:
Received 16 July 2015
Received in revised form 6 December 2015
Accepted 22 March 2016
Available online 31 March 2016

Keywords:
Generalized time-bandwidth product (GTBP)
Fractional S transform
Optimal order
Normalized second-order central moment (NSOCM)
Spectral decomposition
Seismic signal

ABSTRACT

As the extension of time-bandwidth product (TBP) in the fractional domain, the generalized time-bandwidth product (GTBP) provides a rotation-independent measure of compactness. A new fractional S transform (FrST) is proposed to avoid missing the physical meaning of the fractional time–frequency plane. FrST is based on the GTBP criterion and the time–frequency rotation property of fractional Fourier transform (FrFT). In addition, we introduce the normalized second-order central moment (NSOCM) calculation method to determine the optimal order. The optimal order searching process can be converted into the NSOCM calculation. Compared with TBP search algorithms, the NSOCM approach has higher computational efficiency. The qualitative advantage of the NSOCM approach in the optimal order selection is demonstrated by a series of model tests. The optimal FrST based on NSOCM (OFrST) can produce more compact time–frequency support than the S transform. The real seismic data spectral decomposition results show that the proposed algorithm can obtain single-frequency visualization with better time-frequency concentration, thereby enhancing the precision of reservoir prediction.

1. Introduction

Time–frequency analysis is the critical technology of seismic spectral decomposition and plays an important role in the reservoir characterization and fluid recognition. Some of the well-known time–frequency analysis methods include short-time Fourier transform (STFT), Gabor transform (GT), continuous-wavelet transform (CWT) and Wigner–Ville distribution (WVD). Although these time–frequency representations have their own merits, they suffer from low resolution, cross-term interference and other issues. These deficiencies result in an unsatisfactory time–frequency distribution (TFD) for high precision seismic exploration.

The S transform was proposed by Stockwell et al. (1996) as a combination of STFT and CWT. The S transform has the advantage of multi-scale focusing due to the moving local Gaussian window, the scale of which varies with frequency. However, the drawback of S transform is that it has a fixed basic wavelet. To improve the flexibility and time–frequency resolution of S transform, efforts have been made to develop modified S transform by attempting to change the window function with new scaling rule (Roopa and Narasimhan, 2014; Djurović et al., 2008; Sejdic et al., 2008; Stockwell, 2007; Pinnegar and Mansinha, 2003; Mansinha et al., 1997).

Fractional time–frequency analysis (FrTFA), which is a research hotspot in signal processing, has great potential for seismic exploration applications (Jhanwar et al., 2014; Tian and Peng, 2014; Venkitaraman and Seelamantula, 2014; Chen et al., 2013; Irfan et al., 2013; Chen and Peng, 2012; Xu and Guo, 2012; Tao et al., 2010, 2007; Akan and Çekiç, 2003). FrTFA can be considered to be the generalization of a time–frequency representation in the fractional Fourier domain. FrTFA is based on the fractional Fourier transform (FrFT) theory. The form of FrTFA, in general, is defined by adopting the fractional kernel instead of the Fourier transform (FT) kernel. For example, Xu and Guo (2012) replaced the kernel $\exp(-j2\pi ft)$ with a fractional kernel to propose the fractional S transform, which can be regarded as adding a Gaussian window on the FrFT definition formula. According to the rotation property of FrFT (Almeida, 1994), the frequency axis of fractional S transform is a fractional frequency axis, which lies away from the actual frequency. Durak and Arikan (2002, 2003) introduced the generalized time bandwidth product (GTBP) and proposed the GTBP optimal STFT analysis. This approach can ensure that the physical meaning of time–frequency plane is maintained. Chen and Peng (2012) used the GTBP theory to optimize the short-time FrFT. Chen et al. (2013) and Tian and Peng (2014) studied the optimal order searching algorithm of the optimal fractional Gabor transform based on the GTBP criterion.

In fact, the main difficulties of the FrTFA focus on 1) the corresponding relation between fractional frequency and actual frequency and 2) the optimal order selection issue. In this paper, we propose the fractional S transform (FrST), taking advantage of the GTBP definition and the FrFT properties. This representation can avoid the non-

* Corresponding author.
E-mail address: zmpeng@uestc.edu.cn (Z. Peng).

http://dx.doi.org/10.1016/j.jappgeo.2016.03.011
0926-9851/

correspondence between the fractional frequency and the actual frequency. Next, we introduce the normalized second-order central moment (NSOCM) calculation method to directly obtain the optimal order. The strength and advantage of the NSOCM method lies in its non-ergodic search mechanism, which can improve the computing efficiency to a great extent. The obtained FrST representation based on NSOCM (OFrST) is able to effectively solve the above two difficulties of the FrTFA. Different from other modified S transform methods, the OFrST can improve the energy concentration of S transform more flexibly by using FrFT. The performance of the proposed method is assessed on both simulated and real seismic data. The spectral decomposition results show that OFrST can achieve a high time–frequency resolution for a seismic signal. Further, the NSOCM calculation method is also applicable to determine the optimal order of other FrTFA methods.

2. Method

2.1. Fractional Fourier transform

The a-th order FrFT of signal $x(t)$ is defined as

$$x_a(u) = F^a[x(t)] = \int_{-\infty}^{+\infty} K_a(u,t)x(t)dt \tag{1}$$

$$K_a(u,t) = \frac{e^{-j\pi \mathrm{sgn}(\sin\phi)/4+j\phi/2}}{|\sin\phi|^{1/2}} e^{j\pi\left(u^2\cot\phi - 2ut\csc\phi + t^2\cot\phi\right)} \tag{2}$$

where a is the order of FrFT, $0<|a|<2$, $\phi = a\pi/2$ is the corresponding rotation angle of a, and $K_a(u,t)$ is the fractional Fourier transform kernel.

The FrFT has the time shift and frequency shift properties as follows

$$F^a[x(t-\tau)] = e^{j\pi\tau^2 \sin\phi\cos\phi} x_a(u-\tau\cos\phi)e^{-j2\pi u\tau\sin\phi} \tag{3}$$

$$F^a\left[e^{j2\pi tf}x(t)\right] = e^{-j\pi f^2 \sin\phi\cos\phi} x_a(u-f\sin\phi)e^{j2\pi uf\cos\phi} \tag{4}$$

2.2. Fractional S transform

The S transform of signal $x(t)$ is defined as

$$\mathrm{ST}_x(t,f) = \int_{-\infty}^{+\infty} x(\tau)\cdot g(\tau-t,f)\cdot e^{-i2\pi f\tau}d\tau \tag{5}$$

where the Gaussian window is given by

$$g(\tau,f) = \frac{|f|}{\sqrt{2\pi}} e^{-\frac{\tau^2 f^2}{2}} \tag{6}$$

Considering the rotation property of TFD, the fractional S transform (FrST) can be defined as

$$\mathrm{FrST}_x(t,f) = \mathrm{R}_\phi\{\mathrm{ST}_{x_a}(t,f)\} \tag{7}$$

where x_a represents the a-th order FrFT of $x(t)$ and R_ϕ is the rotation operator defined in (8). Using R_ϕ, the fractional time–frequency plane can be rotated back to the original time–frequency plane.

$$\mathrm{R}_\phi = \begin{pmatrix} \cos\phi & \sin\phi \\ -\sin\phi & \cos\phi \end{pmatrix} \tag{8}$$

Using the time shift and frequency shift properties of FrFT, the Eq. (7) becomes

$$\begin{aligned}
|\mathrm{FrST}_x(t,f)| &= \left|\mathrm{R}_\phi\left\{\int_{-\infty}^{\infty} x_a(\tau)\cdot g(\tau-t,f)\cdot e^{-j2\pi f\tau}d\tau\right\}\right| \\
&= \left|\mathrm{R}_\phi\left\{\int_{-\infty}^{\infty}\int_{-\infty}^{\infty} x(t')K_a(t',\tau)dt'\cdot g(\tau-t,f)\cdot e^{-j2\pi f\tau}d\tau\right\}\right| \\
&= \left|\mathrm{R}_\phi\left\{\int_{-\infty}^{\infty} x(t')\cdot\left[\int_{-\infty}^{\infty} g(\tau-t,f)\cdot e^{j2\pi f\tau}\cdot K_{-a}(t',\tau)d\tau\right]^* dt'\right\}\right| \\
&= \left|\mathrm{R}_\phi\left\{\int x\left(t'\right)\cdot\left\{FrFT_{-a}\left[g(\tau-t,f)\cdot e^{j2\pi f\tau}\right]\right\}^* dt'\right\}\right| \\
&= \left|\mathrm{R}_\phi\left\{\int x\left(t'\right)\cdot e^{j\pi\left(t^2-f^2\right)\sin\phi\cos\phi} g^*_{-a}(t'-t\cos\phi+f\sin\phi,f)e^{-j2\pi t'(t\sin\phi+f\cos\phi)}dt'\right\}\right| \\
&= \left|\mathrm{R}_\phi\left\{\mathrm{R}_\phi^{-1}\int x\left(t'\right)\left[g^*_{-a}(t'-t,f)e^{-j2\pi t'f}\right]dt'\right\}\right| \\
&= \left|\int x\left(t'\right)\cdot g_a(t'-t,f)e^{-j2\pi t'f}dt'\right| \quad .
\end{aligned} \tag{9}$$

The derivation process ignores the exponential terms without t', which has no effect on the amplitude. It is obvious that the FrFT operation of signal $x(t)$ is transferred to the window function. The a-th fractional Gaussian window can be written as

$$g_a(u,f) = F^a[g(t,f)] = \sqrt{\frac{f^2(1+j\cot\phi)}{f^2+j2\pi p^2\cot\phi}}\cdot e^{-\pi u^2\frac{j\left(f^4-4\pi^2\right)\cot\phi+2\pi f^2\csc^2\phi}{f^4+4\pi^2\cot^2\phi}}. \tag{10}$$

The FrFT of the Gaussian window is also a Gaussian window with a different shape. Thus, the fractional Gaussian window will not change the time–frequency plane. Hence, the time–frequency plane of FrST is retained in the original plane. And by adding the fractional Gaussian window to the signal, the local spectra representation with high resolution can be obtained.

2.3. NSOCM-based optimal order selection algorithm

The time-bandwidth product (TBP) can be regarded as the evaluation criterion for compactness. Durak and Arikan (2002, 2003) proposed the generalized time-bandwidth product (GTBP), which is the extension of TBP in the fractional domain, defined as

$$\mathrm{GTBP}\{x(t)\} = \min_{0\le a<4}\mathrm{TBP}\{x_a(u)\}. \tag{11}$$

According to the definition of GTBP, the optimal order a_{opt} is normally given by

$$a_{opt} = \arg\min_a \mathrm{TBP}\{x_a(u)\},\quad 0\le a<2. \tag{12}$$

The global search based on minimum TBP requires expensive computation. In this paper, we calculate the NSOCM of the fractional signal $x_a(u)$ to obtain the optimal order. This approach does not require globally searching, improving the computational efficiency of searching process.

The NSOCM p_a of fractional signal $x_a(u)$ is defined by (Alieva and Bastiaans, 2000; Stanković et al., 2003)

$$p_a = \frac{\int_{-\infty}^{\infty}(u-m_a)^2|x_a(u)|^2du}{\int_{-\infty}^{\infty}|x_a(u)|^2du} = w_a - m_a^2 \tag{13}$$

where $m_a = \frac{\int_{-\infty}^{\infty}u|x_a(u)|^2du}{\int_{-\infty}^{\infty}|x_a(u)|^2du}$ is the normalized first-order origin moment of $x_a(u)$, and $w_a = \frac{\int_{-\infty}^{\infty}u^2|x_a(u)|^2du}{\int_{-\infty}^{\infty}|x_a(u)|^2du}$ is the normalized second-order origin moment of $x_a(u)$. The NSOCM p_a and p_{a+1} represent the time width and frequency width of $x_a(u)$, respectively. Hence, Eq. (12) becomes

$$a_{opt} = \arg\min_a\{p_a\cdot p_{a+1}\},\quad 0\le a<1. \tag{14}$$

The NSOCM product is given by

$$p_a \cdot p_{a+1} = p_0 \cdot p_1 + \frac{1}{4}\left[(p_0-p_1)^2 - 4\mu_0^2\right]\sin^2(a\pi) + \frac{1}{2}\mu_0(p_0-p_1)\sin(2a\pi) \quad (15)$$

where $\mu_0 = (w_0+w_1)/2 + m_0m_1 - w_{0.5}$ is the mixed second-order moment. Setting the first derivative of $p_a \cdot p_{a+1}$ with respect to the order a equal zero, we obtain

$$\tan(2a_e\pi) = \frac{4\mu_0(p_0-p_1)}{4\mu_0^2-(p_0-p_1)^2}. \quad (16)$$

For this case where a is equal to the extreme point a_e, the product $p_a \cdot p_{a+1}$ reaches the extremum values. In addition, a constraint condition in Eq. (17) is required to select the minimum point from the extreme points.

$$\left.\frac{d^2(p_a \cdot p_{a+1})}{da^2}\right|_{a=a_e} = 2\pi^2\mu_0(p_1-p_0)/\sin(2a_e\pi) > 0. \quad (17)$$

Although the period of $p_a \cdot p_{a+1}$ is one, the expressions of fractional window at the a-th order and the a + 1-th order are different. This has a great impact on the performance of the optimal fractional S transform representation. In view of this, the calculation range is expanded from [0,1] to [0,2]. This result demonstrates that the product $p_a \cdot p_{a+1}$ reaches its minimum when a satisfies Eq. (18). The calculated results of a are two values with an interval of 1. In addition, we choose the value whose fractional signal has a higher maximal modulus as the final optimal order.

$$\begin{cases} a = \frac{1}{2\pi}\cdot \arctan\left(\frac{4\mu_0(p_0-p_1)}{4\mu_0^2-(p_0-p_1)^2}\right) + \frac{n}{2}, n = 0,1,2,3,4 \\ \mu_0(p_1-p_0)/\sin(2a\pi) > 0 \end{cases} \quad (18)$$

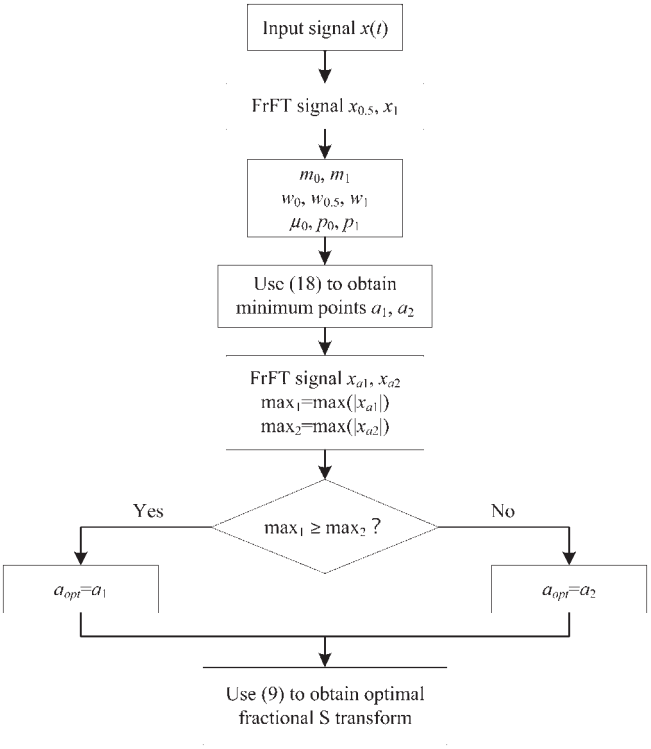

Fig. 1. Flowchart of the OFrST.

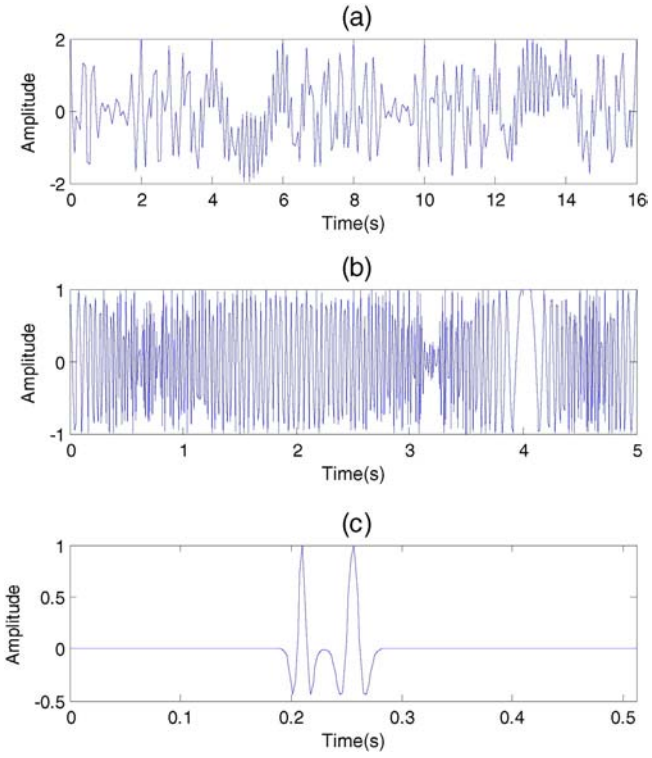

Fig. 2. Synthetic models (a) Model 1; (b) Model 2; (c) Model 3.

2.4. The algorithm flow of the optimal fractional S transform based on NSOCM

The FrST based on NSOCM is referred to as OFrST, and its specific procedures are as follows:

(1) Take the 0.5-th and 1-th order FrFT of signal $x(t)$ to obtain $x_{0.5}$,x_1;
(2) Calculate the normalized first-order origin moments m_0 and m_1; the normalized second-order origin moments w_0, $w_{0.5}$ and w_1; the mixed second-order moment μ_0; and NSOCM p_0 and p_1 in accordance with the definition;
(3) Obtain two values a_1, a_2 of a by using Eq. (18) in the range of [0,2];
(4) Take the a_1-th and a_2-th order FrFT of signal $x(t)$ to obtain x_{a1} and x_{a2}; in addition, obtain the maximal modulus of x_{a1} andx_{a2}, i.e., $\max_1 = \max(|x_{a1}|)$ and$\max_2 = \max(|x_{a2}|)$, respectively;
(5) Compare $\max_1$ and$\max_2$. If $\max_1 > \max_2$, then choose a_1 as the optimal order a_{opt}; otherwise, a_2 becomes the optimal order a_{opt};
(6) Obtain the OFrST representation by Eq. (9).

The flowchart of OFrST is shown in Fig. 1.

3. Simulation test

Synthetic models are generated to test the performance of the proposed method. The ratio L_4/L_2 of the TFD serves as a concentration measure, with a higher ratio corresponding to an improved concentration (Jones and Parks, 1990). In this paper, we consider the L_4/L_2 ratio as

Table 1
Optimal order selection results.

Models	Model 1	Model 2	Model 3
TBPS	1.52	0.44	1
NSOCM calculation	1.5054	0.4825	1

Table 2
Computation time of different optimal order selection methods.

Models	Model 1	Model 2	Model 3
TBPS (ms)	330.49	350.47	371.31
NSOCM calculation (ms)	12.69	12.88	13.16

the TFD's concentration evaluation criterion. In addition, the TBP search (TBPS) is given for comparison with the NSOCM algorithm.

Fig. 2 shows the real part of three test models. Model 1 (Fig. 2(a)) is a multi-component signal that is composed of two frequency-modulated (LFM) signals $x_1(t) = e^{j\pi(t^2-10t)} + e^{j\pi(t^2+5t)}$. Model 2 (Fig. 2(b)) is a nonlinear frequency-modulated (NLFM) signal $x_2(t) = e^{j\pi(12t^3-70t2+180t)}$. Model 3 (Fig. 2(c)) consists of 35 Hz and 50 Hz Ricker wavelets.

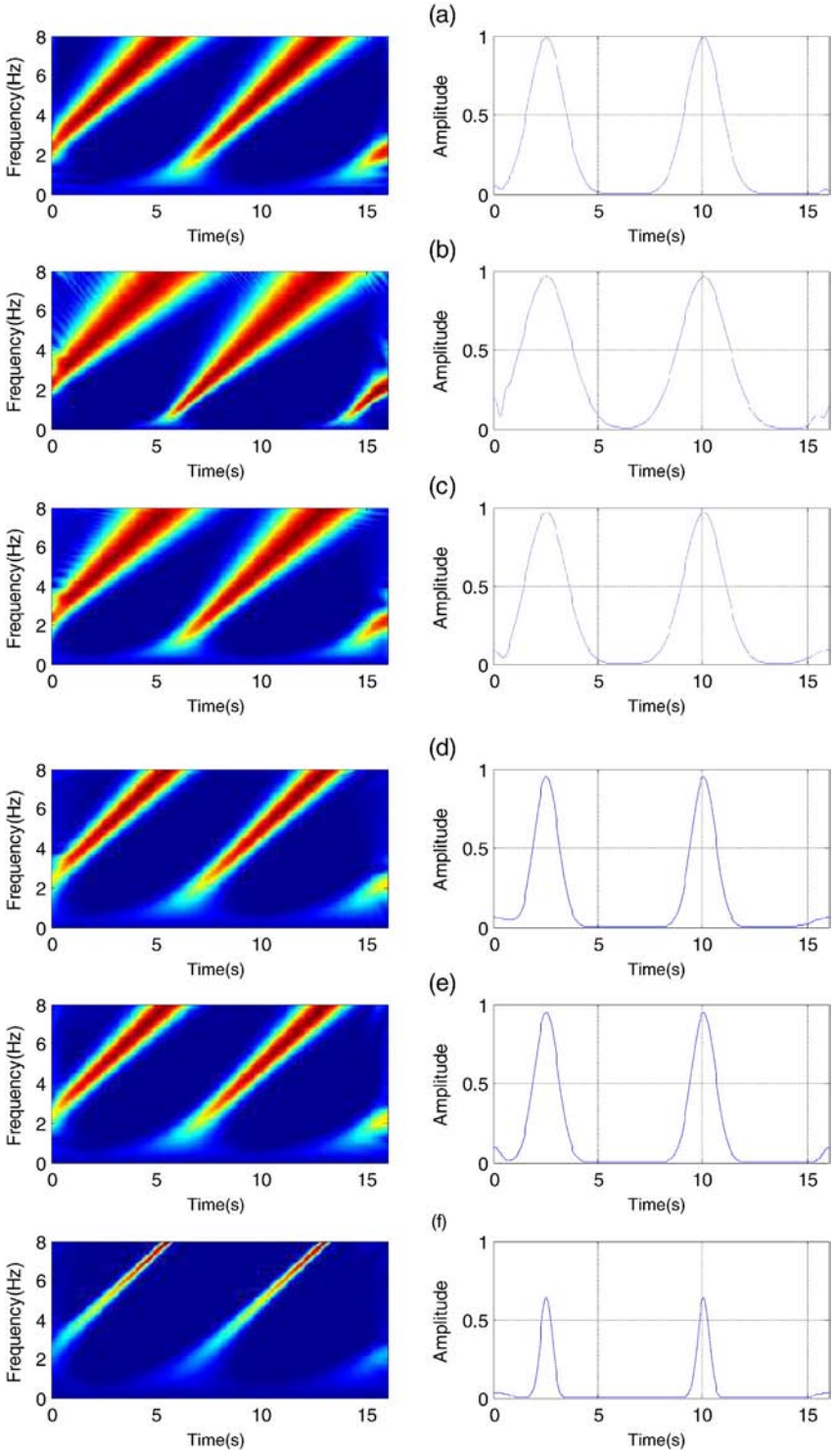

Fig. 3. Model 1's FrST representation and its 5 Hz slices. (a) S transform and its 5 Hz slice; (b) FrST ($a = 0.4$) and its 5 Hz slice; (c) FrST ($a = 0.9$) and its 5 Hz slice; (d) FrST ($a = 1.2$) and its 5 Hz slice; (e) FrST ($a = 1.8$) and its 5 Hz slice; (f) OFrST ($a = 1.5054$) and its 5 Hz slice.

Table 3
L_4/L_2 values of the TFDs in Fig. 3.

TFDs	L_4/L_2
S transform	0.1083
FrST ($a = 0.4$)	0.1016
FrST ($a = 0.9$)	0.1053
FrST ($a = 1.2$)	0.1180
FrST ($a = 1.8$)	0.1181
OFrST ($a = 1.5054$)	0.1528

Table 4
L_4/L_2 values of the TFDs in Fig. 4.

TFDs	L_4/L_2
S transform	0.1146
FrST ($a = 0.2$)	0.1208
FrST ($a = 0.7$)	0.1382
FrST ($a = 1.2$)	0.1238
FrST ($a = 1.8$)	0.1131
OFrST ($a = 0.4825$)	0.1464

Table 1 shows the optimal order selection results of the synthetic models. The optimal order calculated by NSOCM is very close to the TBPS's results, and the computation time of these methods is given in Table 2. It is obvious that the NSOCM calculation greatly reduces the computation time of TBPS. As seen from these results, the NSOCM algorithm can give a reasonable optimal order for the FrST and has the advantage of high computational efficiency.

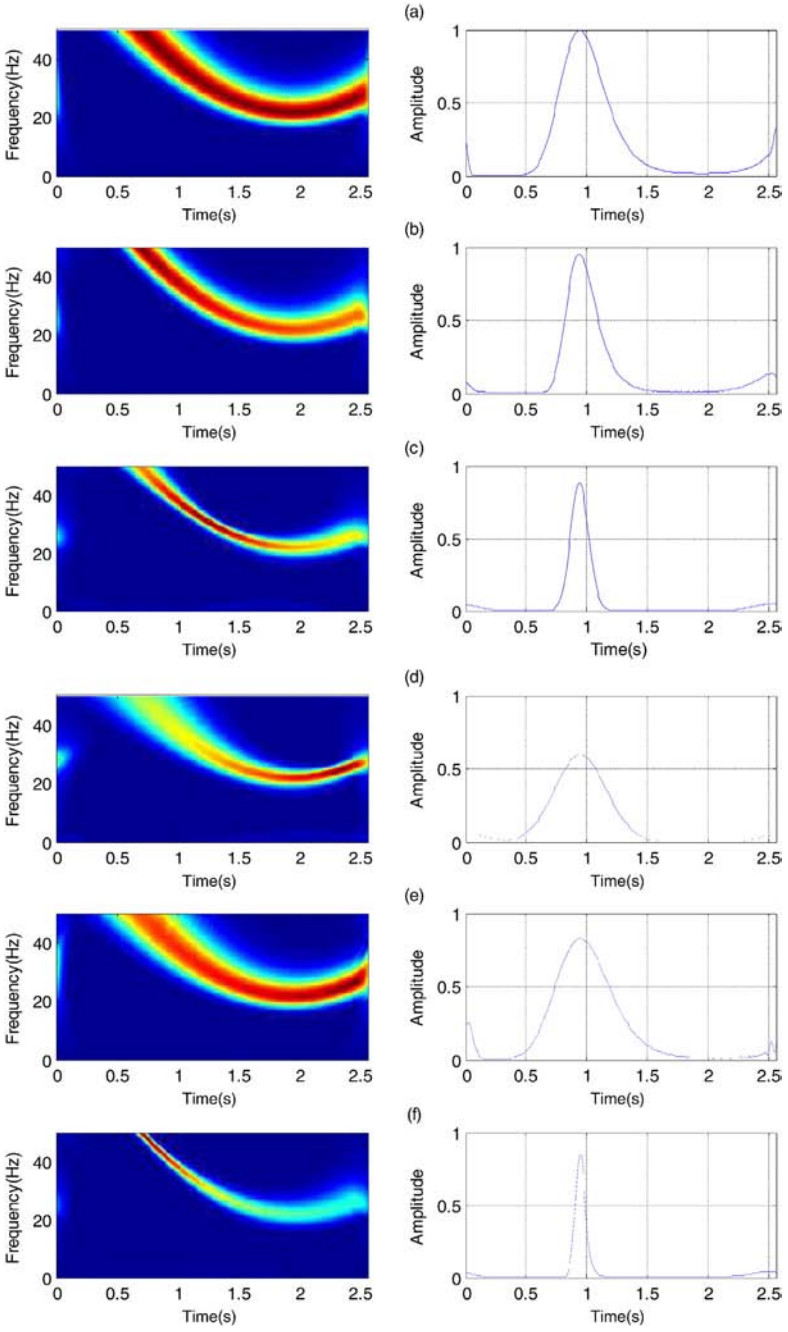

Fig. 4. Model 2′s FrST representation and its 40 Hz slices. (a) S transform and its 40 Hz slice; (b) FrST ($a = 0.2$) and its 40 Hz slice; (c) FrST ($a = 0.7$) and its 40 Hz slice; (d) FrST ($a = 1.2$) and its 40 Hz slice; (e) FrST ($a = 1.8$) and its 40 Hz slice; (f) OFrST ($a = 0.4825$) and its 40 Hz slice.

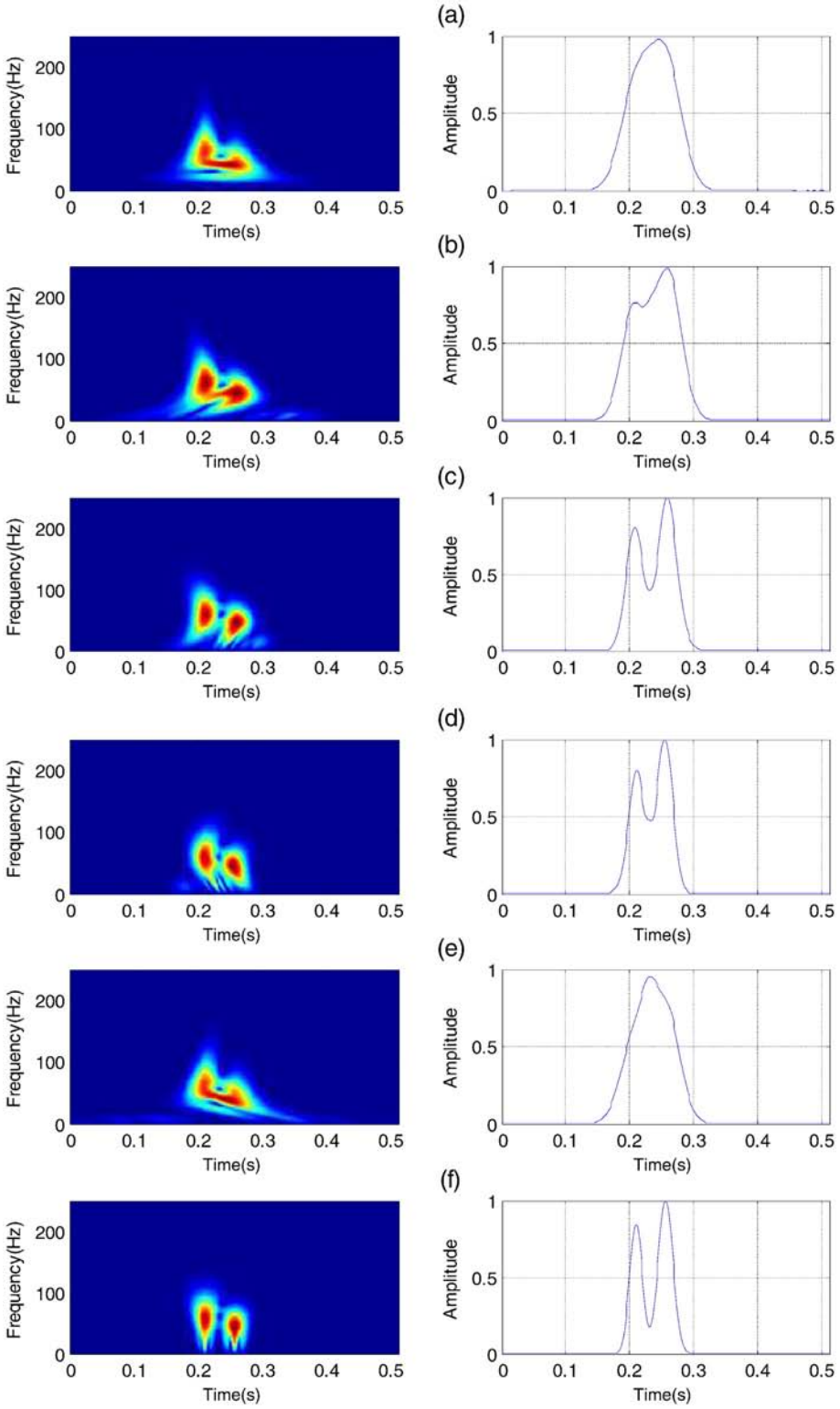

Fig. 5. Model 3′s FrST representation and its 45 Hz slices. (a) S transform and its 45 Hz slice; (b) FrST ($a = 0.3$) and its 45 Hz slice; (c) FrST ($a = 0.6$) and its 45 Hz slice; (d) FrST ($a = 1.3$) and its 45 Hz slice; (e) FrST ($a = 1.8$) and its 45 Hz slice; (f) OFrST ($a = 1$) and its 45 Hz slice.

To better display the good performance of the OFrST representation, we show some specific comparison figures and data. The Model 1′s FrST representations and its 5 Hz slices are shown in Fig. 3. The OFrST (Fig. 3(f)) has a higher time–frequency resolution than S transform (Fig. 3(a)) and the other FrST distributions (Fig. 3(b)–(e)). In addition, the OFrST has the shortest span of the LFM component at $f = 5$ Hz. The comparison of the 5 Hz slices indicates that the OFrST representation is the optimal TFD at this frequency instant. Table 3 lists the L_4/L_2 values of these TFDs. The L_4/L_2 values indicate that the OFrST produces the best performance on the concentration compared to other TFDs.

Table 5
L_4/L_2 values of the TFDs in Fig. 5.

TFDs	L_4/L_2
S transform	0.1661
FrST ($a = 0.3$)	0.1632
FrST ($a = 0.6$)	0.1716
FrST ($a = 1.3$)	0.1753
FrST ($a = 1.8$)	0.1680
OFrST ($a = 1$)	0.1820

Model 2′s FrST representations and the corresponding L_4/L_2 ratio values are given in Fig. 4 and Table 4, respectively. As seen from these results, the OFrST representation gives an optimal TDF with high time–frequency concentration.

Fig. 5 represents Model 3′s FrST representations and its 45 Hz slices. We see that two wavelets interfere with each other in the ST spectrum (Fig. 5(a)). The interference degree of the two wavelets varies with the fractional order of FrST, as shown in the 45 Hz slices. When the fractional order reaches the optimal order, two wavelets can be successfully separated from each other. In addition, Table 5 shows that the time–frequency concentration of OFrST representation is superior to the other TFDs. The simulation test results show the validity and high efficiency of the NSOCM algorithm for optimal order selection, and indicate that the proposed OFrST can significantly improve the time–frequency resolution of S transform.

4. Real seismic data application

The real seismic data are used to verify the feasibility of the proposed method applied in seismic exploration. A single seismic section is shown in Fig. 6(a), and (b) and (c) represent the spectrum of S transform and OFrST, respectively. The L_4/L_2 values of these TFDs are given in Table 6. As seen from these figures and data, the time–frequency spectrum with a high concentration is achieved by adopting OFrST.

Table 6
L_4/L_2 values of the TFDs in Fig. 6.

TFDs	L_4/L_2
S transform	0.1461
OFrST based on NSOCM	0.1738

Fig. 7 shows a seismic section derived from the northeast region of Sichuan basin. The logging information shows that the seismic section from 1800 to 2400 ms is the target stratum for seismic interpretation. In the figure, the sample time is 1800–2400 ms as the ordinate, and the CDP is 300–700 as the abscissa. The seismic section contains 401 seismic traces, with the sampling interval of 2 ms.

The spectral decomposition results of seismic data can be used for reservoir characterization and fluid recognition. Fig. 8 shows the 25 Hz, 30 Hz, 40 Hz and 45 Hz single-frequency slices extracted using the S transform. The structural features in these single-frequency slices are scattered and unclear. To improve the performance of S transform in the seismic data analysis, the single-frequency slices extracted by OFrST are given in Fig. 9. It is obvious that the spectral decomposition results of the proposed method have a higher time–frequency resolution and concentration than those of the S transform. From Fig. 9, we can see that the 40 Hz and 45 Hz single-frequency attributions have obvious energy attenuation, which is consistent with the actual reservoir information. The spectral decomposition results of the proposed method are clearly suitable for seismic interpretation. The proposed method has a good performance of time–frequency resolution and is able to enhance the precision of seismic reservoir prediction.

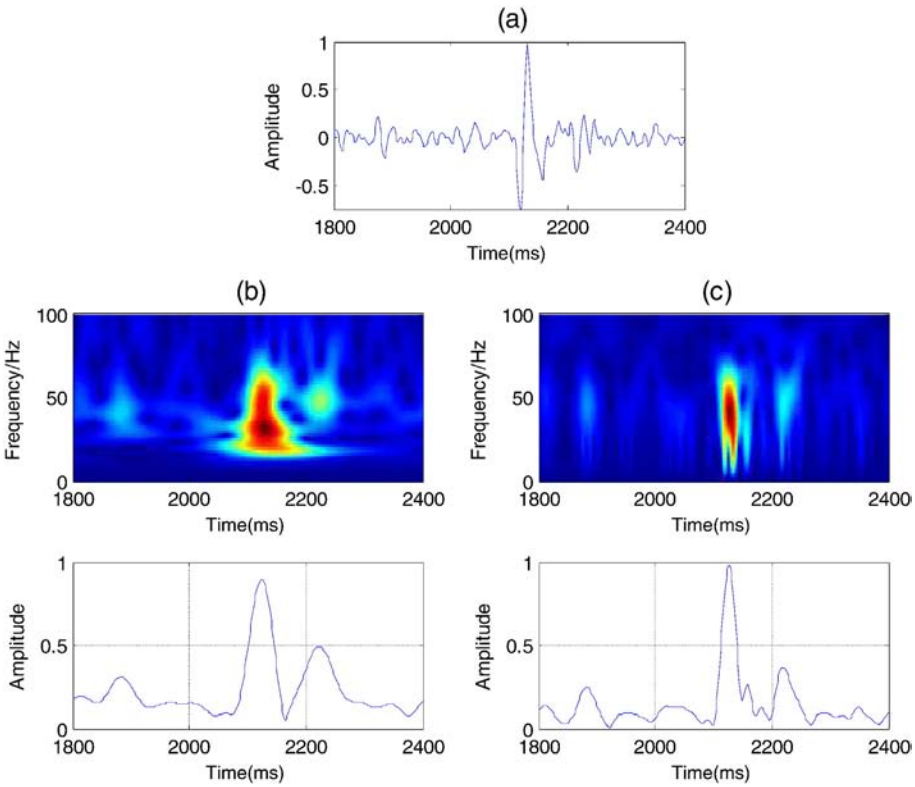

Fig. 6. Single seismic signal and its TFDs (a) Single seismic signal; (b) S transform and its 45 Hz slice; (c) OFrST and its 45 Hz slice.

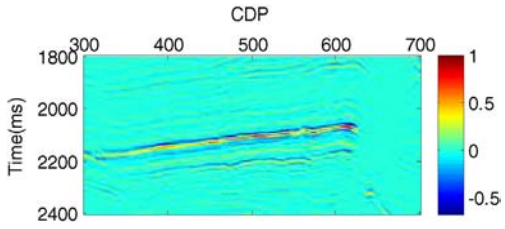

Fig. 7. 2-D seismic data.

5. Conclusions

In this paper, we proposed an optimal FrST based on the NSOCM calculation method to improve the time–frequency resolution of S transform. The theory of OFrST is derived from the GTBP criterion and the properties of FrFT. This representation preserves the physical meaning of fractional time–frequency plane, and obtains a more compact time–frequency support. In addition, the NSOCM calculation algorithm was introduced to find the optimal order. The non-ergodic search mechanism of the NSOCM algorithm can greatly reduce the computational complexity of the optimal order searching process. The advantages of the algorithm of high accuracy and computational efficiency were revealed via comparison with other optimal order searching algorithms.

Testing simulated and real seismic data demonstrated the effectiveness and the superior performance of the proposed method. The spectral decomposition results with a high concentration were achieved by the proposed method for providing more precise structural features, which can promote the application of S transform in reservoir prediction and fluid identification.

The different experiments showed that the NSOCM algorithm is an alternative and suitable approach for the optimal order selection issue. In addition, the algorithm has many potential applications in the other FrTFA, which will be considered in future works.

Acknowledgments

This work is supported by the National Natural Science Foundation of China under grants no. 61571096, no. 41274127 and no. 41301460.

References

Akan, A., Çekiç, Y., 2003. A fractional Gabor expansion. J. Frankl. Inst. 340 (5), 391–397.
Alieva, T., Bastiaans, M.J., 2000. On fractional Fourier transform moments. IEEE Signal Process Lett. 7 (11), 320–323.
Almeida, L.B., 1994. The fractional Fourier transform and time–frequency representations. IEEE Trans. Signal Process. 42 (11), 3084–3091.
Chen, Y.P., Peng, Z.M., 2012. A novel optimal STFrFT and its application in seismic signal processing. Proceedings of the IEEE International Conference on Computational Problem-Solving, pp. 328–331.
Chen, Y.P., Peng, Z.M., He, Z.H., et al., 2013. The optimal fractional Gabor transform based on the adaptive window function and its application. Appl. Geophys. 10 (3), 305–313.

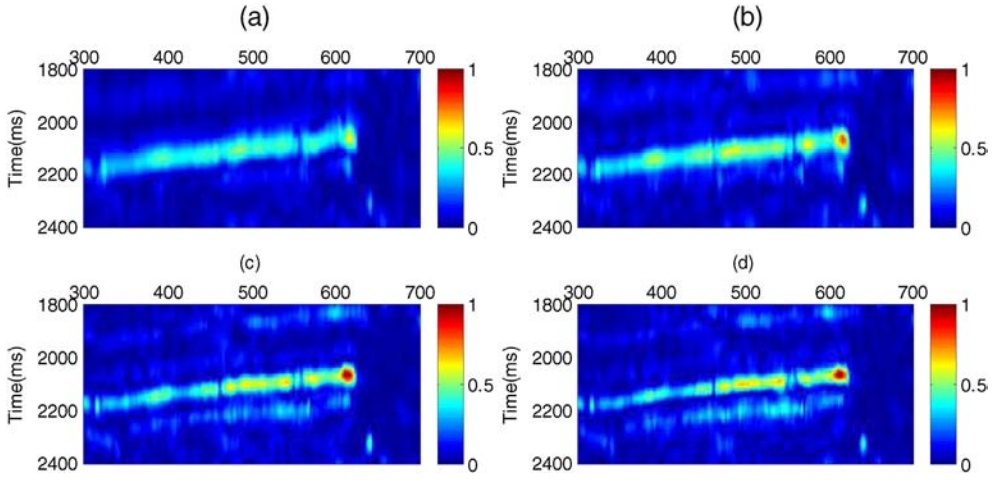

Fig. 8. Single-frequency sections extracted using the S transform (a) 25 Hz; (b) 30 Hz; (c) 40 Hz; (d) 45 Hz.

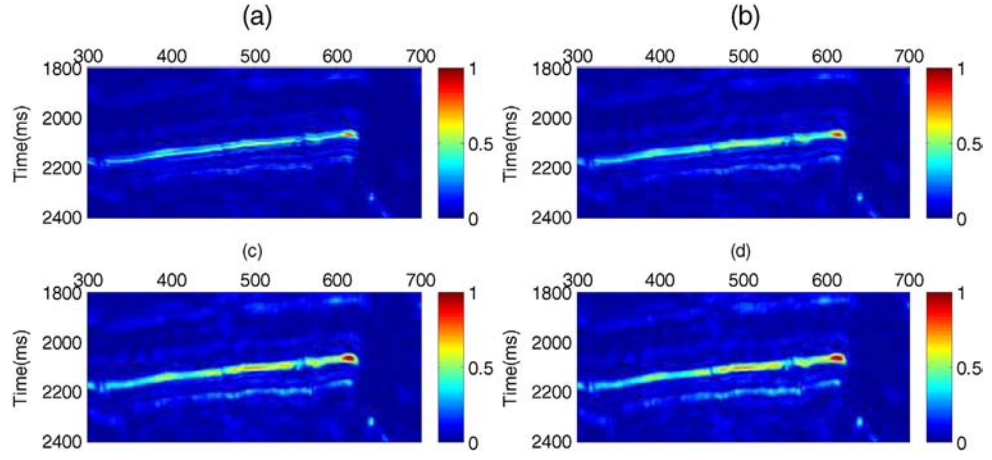

Fig. 9. Single-frequency sections extracted via OFrST based on NSOCM (a) 25 Hz; (b) 30 Hz; (c) 40 Hz; (d) 45 Hz.

Djurović, I., Sejdić, E., Jiang, J., 2008. Frequency-based window width optimization for S-transform. AEU Int. J. Electron. Commun. 62 (4), 245–250.
Durak, L., Arikan, O., 2002. Generalized time bandwidth product optimal short time Fourier transformation. Proceedings of the IEEE International Conference on Acoustics, Speech, and Signal Processing. Vol. 2, pp. 1465–1468.
Durak, L., Arikan, O., 2003. Short-time Fourier transform: two fundamental properties and an optimal implementation. IEEE Trans. Signal Process. 51 (5), 1231–1242.
Irfan, M., Zheng, L., Shahzad, H., 2013. Review of computing algorithms for discrete fractional Fourier transform. Res. J. Appl. Sci. Eng. Technol. 6 (11), 1911–1919.
Jhanwar, D., Sharma, K.K., Modani, S.G., 2014. Generalized fractional S-transform and its application to discriminate environmental background acoustic noise signals. Acoust. Phys. 60 (4), 466–473.
Jones, D.L., Parks, T.W., 1990. A high resolution data-adaptive time–frequency representation. IEEE Trans. Acoust. Speech Signal Process. 38 (12), 2127–2135.
Mansinha, L., Stockwell, R.G., Lowe, R.P., et al., 1997. Local S-spectrum analysis of 1-D and 2-D data. Phys. Earth Planet. Inter. 103, 329–336.
Pinnegar, C.R., Mansinha, L., 2003. The S-transform with windows of arbitrary and varying shape. Geophysics 68 (1), 381–385.
Roopa, S., Narasimhan, S.V., 2014. S-transform based on analytic discrete cosine transform for time–frequency analysis. Signal Process. 105, 207–215.
Sejdic, E., Djurovic, I., Jiang, J., 2008. A window width optimized S-transform. EURASIP J. Adv. Signal Process. 59.
Stanković, L.J., Alieva, T., Bastiaans, M.J., 2003. Time–frequency signal analysis based on the windowed fractional Fourier transform. Signal Process. 83 (11), 2459–2468.
Stockwell, R.G., 2007. A basis for efficient representation of the S-transform. Digital Signal Processing. 17 (1), 371–393.
Stockwell, R.G., Mansinha, L., Lowe, R.P., 1996. Localization of the complex spectrum: the S transform. IEEE Trans. Signal Process. 44 (4), 998–1001.
Tao, R., Li, B.Z., Wang, Y., 2007. Spectral analysis and reconstruction for periodic nonuniformly sampled signals in fractional Fourier domain. IEEE Trans. Signal Process. 55 (7), 3541–3547.
Tao, R., Li, Y.L., Wang, Y., 2010. Short-time fractional Fourier transform and its applications. IEEE Trans. Signal Process. 58 (5), 2568–2580.
Tian, L., Peng, Z.M., 2014. Determining the optimal order of fractional Gabor transform based on kurtosis maximization and its application. J. Appl. Geophys. 108, 152–158.
Venkitaraman, A., Seelamantula, C.S., 2014. Fractional Hilbert transform extensions and associated analytic signal construction. Signal Process. 94, 359–372.
Xu, D.P., Guo, K., 2012. Fractional S transform—part 1: theory. Appl. Geophys. 9 (1), 73–79.